Synthesis and Photovoltaic Properties of D–A Copolymers Based on Dithienosilole and Benzotriazole

6 AUTHORS, INCLUDING:

Jie Min
Institute Materials for Electronics and Energ…
46 PUBLICATIONS **1,156** CITATIONS

SEE PROFILE

Siyuan Zhang
Georgia Institute of Technology
15 PUBLICATIONS **362** CITATIONS

SEE PROFILE

Maojie Zhang
Soochow University (PRC)
64 PUBLICATIONS **2,440** CITATIONS

SEE PROFILE

Jing Zhang
Fourth Military Medical University
**689** PUBLICATIONS **10,054** CITATIONS

SEE PROFILE

Synthesis and Photovoltaic Properties of D−A Copolymers Based on Dithienosilole and Benzotriazole

Jie Min, Zhi-Guo Zhang,* Siyuan Zhang, Maojie Zhang, Jing Zhang, and Yongfang Li*

Beijing National Laboratory for Molecular Sciences, CAS Key Laboratory of Organic Solids, Institute of Chemistry, Chinese Academy of Sciences, Beijing 100190, China

ABSTRACT: Two new donor−acceptor (D−A) copolymers containing dithienosilole (DTS) donor unit and benzotriazole (BTA) acceptor unit without and with thiophene bridge, PDTS-BTA and PDTS-DTBTA, were synthesized to study their structure−property relationships for the application in polymer solar cells (PSCs). Compared to PDTS-BTA, adding thiophene bridges in PDTS-DTBTA improves planarity and increases effective conjugation of the polymer main chain, which translated into broader and stronger absorption, higher hole mobility, and better photovoltaic performance. Under the illumination of AM1.5G, 100 mW/cm^2, the PSC based on PDTS-DTBTA/PC$_{70}$BM demonstrated a power conversion efficiency of 3.80%, which is significantly improved in comparison with that (1.64%) of the device based on PDTS-BTA/PC$_{70}$BM under the same experimental conditions.
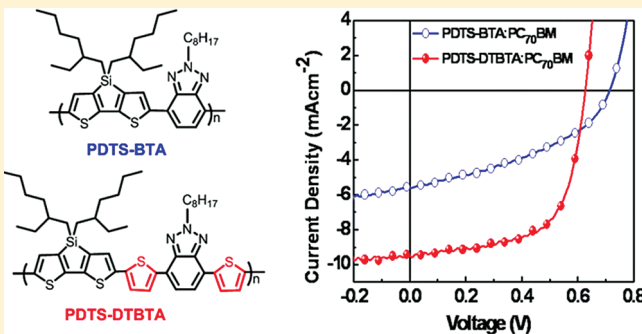
INTRODUCTION

Bulk heterojunction (BHJ) polymer solar cells (PSCs) based on p-type conjugated polymers as donor and n-type fullerene derivatives as acceptor have been intensively studied in recent years for the generation of affordable, clean, and renewable energy.[1] Advantages of the BHJ PSCs include low-cost fabrication of large-area devices, light weight, mechanical flexibility, and easy tunability of chemical properties of the photovoltaic materials.

It has been realized that an ideal polymer donor in PSCs should exhibit broad absorption with high absorption coefficient in the visible region, high hole mobility, suitable energy level matching to the fullerene acceptor, and appropriate compatibility with fullerene acceptor to form nanoscale bicontinuous interpenetrating network. All these specific design criteria can offer high values of short-circuit current (J_{sc}), open-circuit voltage (V_{oc}), and fill factor (FF) of the PSCs, all of which are related to the power conversion efficiency (PCE).[2,3] One feasible approach toward broadening the visible absorption and tuning the energy levels is to design alternating donor−acceptor (D−A) copolymers, in which the orbital mixing of the donor moiety and the acceptor moiety provides a means for narrowing the bandgap and tuning the energy levels of conjugated polymers.[4−16]

In such polymers, electron-rich units such as carbazole,[17] benzodithiophene,[18] indacenodithiophene,[19,20] dithieno[3,2-b:2′,3′-d]silole,[21,22] benzobis(silolothiophene),[23,24] and cyclopenta[2,1-b:3,4-b′]dithiophene[25] have been developed as donor units, while diketopyrrolo[3,4-c]-pyrrole-1,4-dione,[26,27] benzothiadiazole,[28−30] quinoxaline,[31] thieno[3,4-c]pyrrole-4,6-dione,[32−35] and their derivatives have been commonly used as electron acceptor units.

Among the acceptors, benzothiadiazole is one of the most successfully and widely used acceptors. Replacing of the sulfur atom with nitrogen atom affords benzotriazole (BTA), which can provide an additional advantage of incorporating solubilizing alkyl chains onto the acceptor unit, rather than on the thiophene rings of the polymer.[36] This unique distribution of the alkyl chains allows the polymer backbone to adopt a more planar conformation, which can promote close packing of the polymer chain and increase the hole mobility of the resulting polymer. Along these lines, copolymers of benzotriazole with electron-denoting group of carbazole,[37] fluorene,[38] and benzodithiophene[39,40] have been well developed in the past two years. With the above-mentioned merit in mind, one must aware that the lone pair on the nitrogen atom also weakened the electron-acceptor ability of benzotriazole. In the reported BTA-based polymers, the donor units are based on fluorine, carbazole, or benzene fused thiophene structure. Because of the weak electron-donating nature of the benzene units, their copolymers with BTA weak acceptor unit show large bandgap and poorer absorption.

Obviously, a stronger electron-donating unit is needed to reduce the bandgap and broaden the absorption of the BTA-based copolymers. Among the donor units reported, dithieno-[3,2-b:2′,3′-d]silole (DTS) could be an appropriate choice of such strong donor units. Further considering the higher hole mobility and the lower LUMO energy level of the copolymers containing DTS unit,[21,41] here we synthesized two new D−A

Scheme 1. Synthetic Route for the Copolymers[a]
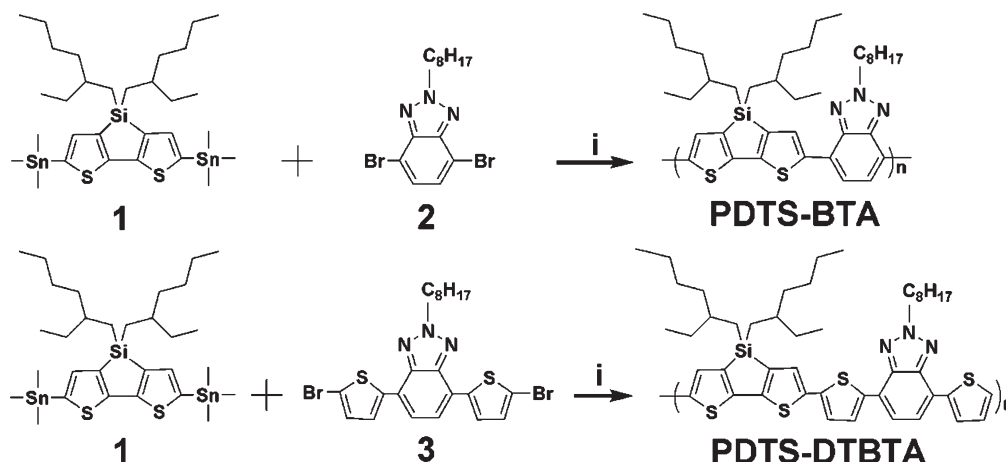
[a] Reagents and conditions: (i) Pd(PPh$_3$)$_4$, toluene, 120 °C, argon.

copolymers containing DTS donor unit and BTA acceptor unit, PDTS-BTA and PDTS-DTBTA (see Scheme 1). The difference of the two polymers is the thiophene bridges between the donor and acceptor units in PDTS-DTBTA. The polymers do show narrower bandgap and broader absorption in the visible region, and PDTS-DTBTA displays further improved absorption. The effect of thiophene bridges on absorption, morphology, mobility, and photovoltaic properties of the copolymers was fully investigated in this paper.

■ EXPERIMENTAL SECTION

Materials. All chemicals and solvents were reagent grade and purchased from Aldrich, Alfa Aesar, and TCI Chemical Co. Toluene, tetrahydrofuran, and diethyl ether were distilled to keep anhydrous before use. The other solvents were degassed by nitrogen prior to use, unless otherwise stated.

Measurements. All new compounds were characterized by ^{1}H NMR. Nuclear magnetic resonance (NMR) spectra were measured on a Bruker DMX-400 spectrometer. Chemical shifts of the ^{1}H NMR were reported in ppm relative to the singlet of CDCl$_3$ at 7.26 ppm. Splitting patterns were designated as s (singlet), d (doublet), t (triplet), m (multiplet), and br (broad). The molecular weight of the polymers was measured by gel permeation chromatography (GPC), and polystyrene was used as a standard. Thermogravimetric analysis (TGA) was performed on a Perkin-Elmer TGA-7. Absorption spectra were taken on a Hitachi U-3010 UV–vis spectrophotometer. The electrochemical cyclic voltammetry was conducted on a Zahner IM6e electrochemical workstation.

Charge carrier mobility in blend films was measured by space charge limited current (SCLC) method. The hole-only devices with the same active layer thickness as that in PSCs were fabricated with an ITO/PEDOT:PSS/polymer:PCBM(1:1)/Au structure. The hole mobility was calculated by fitting the dark $J–V$ curves for the hole-only devices to SCLC model at low voltages, in which the current density is given by $J = 9\varepsilon_0\varepsilon_r\mu V^2/8L^3 \exp[0.891\gamma(V/L)^{0.5}]$, where $\varepsilon_0\varepsilon_r$ represents the permittivity of the material, μ is the mobility, γ is the field activation factor, and L is the thickness of the active layer. The applied bias voltage is corrected for the built-in potential so that $V = V_{\text{applied}} - V_{\text{bi}}$.

Fabrication and Characterization of PSCs. PSCs were fabricated with ITO glass as a positive electrode, Ca/Al as a negative electrode, and the blend film of the polymer/PC$_{70}$BM between them

as a photosensitive layer. The ITO glass was precleaned and modified by a thin layer of PEDOT:PSS which was spin-cast from a PEDOT:PSS aqueous solution (Clevious P VP AI 4083 H. C. Stark, Germany) on the ITO substrate, and the thickness of the PEDOT:PSS layer is about 30 nm. The photosensitive layer was prepared by spin-coating a blend solution of polymers and PC$_{70}$BM in o-dichlorobenzene on the ITO/PEDOT:PSS electrode. Then the Ca/Al cathode was deposited on the polymer layer by vacuum evaporation under 3×10^{-5} Pa. The thickness of the photosensitive layer is ca. 80 nm, measured on an Ambios Tech. XP-2 profilometer. The effective area of one cell is 4 mm^2. The current–voltage ($J–V$) measurement of the devices was conducted on a computer-controlled Keithley 236 source measure unit. A xenon lamp with AM1.5 filter was used as the white light source, and the optical power at the sample was 100 mW cm^{-2}.

Synthesis of the Monomers and Polymers. The following compounds were synthesized according to the procedure in the literature: 4,4′-bis(2-ethylhexyl)-5,5′-bis(trimethyltin)dithieno[3,2-b:2′,3′-d]silole (**1**),[21] 4,7-dibromo-2-octylbenzotriazole (**2**),[37] and 2-octyl-4,7-di(5-bromothiophen-2-yl)-2H-benzo[1,2,3]triazole (**3**).[37,40] The synthetic routes of the copolymers are shown in Scheme 1. The detailed synthetic processes are as follows.

Poly{4,4′-bis(2-ethylhexyl)dithieno[3,2-b:2′,3′-d]silole-5,5′-diyl-alt-2-octyl-1,2,3-benzotriazole-4,7-diyl} (PDTS-BTA). Under the protection of argon atmosphere, 0.5 mmol of monomer **1** was put into a two-neck flask. Then 12 mL of degassed toluene and 0.5 mmol of monomer **2** were added to the mixture. The solution was flushed with argon for 10 min, and then 25 mg of Pd(PPh$_3$)$_4$ was added. After another flushing with argon for 20 min, the reactant was heated to reflux for 24 h. Then the reactant was cooled to room temperature, and the polymer was precipitated by adding 200 mL of methanol, filtered through a Soxhlet thimble, and then subjected to Soxhlet extraction with methanol, hexane, and chloroform. The polymer was recovered as solid from the chloroform fraction by rotary evaporation. The solid was dried under vacuum for 12 h to get PDTS-BTA. The yield of the polymerization reaction was about 63%. GPC: M_w = 13.9 kg mol^{-1}, M_n = 6.7 kg mol^{-1}, M_w/M_n = 2.07. ^{1}H NMR (400 MHz, CDCl$_3$), δ (ppm): 8.11 (br, 2H), 7.64–7.47 (m, 2H), 4.87 (s, 2H), 2.26 (s, 2H), 1.58–1.02 (m, 40H), 0.89–0.83 (m, 18H). The elemental analysis results of PDTS-BTA are as follows: Calculated: C, 69.62; H, 8.40; S, 9.77; N, 7.33. Found: C, 69.73; H, 8.51; S, 9.66; N, 7.38.

Poly{4,4′-bis(2-ethylhexyl)dithieno[3,2-b:2′,3′-d]silole-5,5′-diyl-alt-5,8-di(thien-2-yl)-2-octyl-1,2,3-benzotriazole-5,5′-diyl} (PDTS-DTBTA). The polymerization process was the same as that for PDTS-BTA, except that

Table 1. Molecular Weights and Thermal Properties of the Polymers

polymers	$M_w{}^a$	$M_n{}^a$	PDI^a	T_d (°C)^b
PDTS-BTA	13.9K	6.7K	2.07	388
PDTS-DTBTA	14.4K	8.0K	1.80	415

^{a} M_n, M_w, and PDI of the polymers were determined by GPC using polystyrene standards in THF. ^{b} The 5% weight-loss temperatures under inert atmosphere.
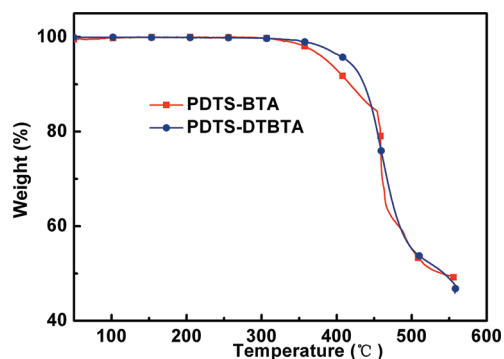
Figure 1. TGA plots of the polymers with a heating rate of 10 °C min^{-1} under an inert atmosphere.

monomer **3** was used instead of monomer **2** and the reactant was refluxed for 15 h. The yield of the polymerization reaction was about 55%. GPC: M_w = 14.4 kg mol^{-1}, M_n = 8.0 kg mol^{-1}, M_w/M_n = 1.80. ^{1}H NMR (400 MHz, CDCl$_3$), δ (ppm): 8.13 (br, 2H), 7.60−7.43 (m, 4H), 4.85 (s, 2H), 2.23 (s, 8H), 1.56−1.25 (m, 36H), 1.02−0.88 (m, 18H). The elemental analysis results of PDTS-DTBTA are as follows: Calculated: C, 67.40; H, 7.20; S, 15.63; N, 6.35. Found: C, 68.02; H, 7.31; S, 15.25; N, 6.17.

■ RESULTS AND DISCUSSION

Synthesis and Thermal Stability. Synthetic routes of the polymers are outlined in Scheme 1. The two copolymers PDTS-BTA and PDTS-DTBTA were synthesized by Stille coupling reaction.[42] All the two polymers have good solubility in common organic solvents such as chloroform, toluene, and chlorobenzene. Molecular weights and polydispersity indices (PDIs) of the polymers, as shown in Table 1, are determined by gel permeation chromatography (GPC) analysis with a polystyrene standard calibration. Molecular weight of the polymers was determined by gel permeation chromatography (GPC). The M_n's of PDTS-BTA and PDTS-DTBTA were found to be 6.7×10^3 and 8.0×10^3 g/mol, respectively, with the corresponding polydispersity indices of 2.07 and 1.80.

Thermal stability of the polymers was investigated with thermogravimetric analysis (TGA), as shown in Figure 1. The TGA analysis reveals that the onset temperatures with 5% weight loss (T_d) of PDTS-BTA and PDTS-DTBTA are 388 and 415 °C, respectively. This indicates that the copolymers is stable enough for the applications in optoelectronic devices.

Optical Properties. Figure 2 shows the absorption spectra of PDTS-BTA and PDTS-DTBTA in chloroform solution and in solid film. The corresponding data are summarized in Table 2. The solution absorption spectra of PDTS-BTA and

PDTS-DTBTA show similar profile with the absorption maxima at 567 and 575 nm, respectively. The spectral red shift for PDTS-DTBTA solution could be attributed to its planar backbone, benefiting from reduced steric hindrance by insertion of the thiophene bridges. The advantage of adding the thiophene bridges is also revealed by molar extinction coefficient, as shown in Figure 2b. The absorbance per unit thickness of PDTS-DTBTA film at maximum absorption reached 0.6×10^{-2}/nm, much higher than that (0.5×10^{-2}/nm) of PDTS-BTA film. Compared to PDTS-BTA, the broader and stronger absorption feature for PDTS-DTBTA is beneficial to its photoharvesting when it is used as donor material in PSCs. The absorption spectra of the polymer films, as also shown in Figure 2b, red-shifted than that of the polymer solutions, which is a common phenomenon due to the polymer main chain aggregation and interactions in the solid film.[43] In addition, there are stronger shoulder peaks in the long wavelength direction of the polymer film absorption spectra, indicating that there exist some ordered structure in the polymer films, which should benefit higher hole mobility and photovoltaic performance of the polymers.[44] The absorption edges of PDTS-BTA and PDTS-DTBTA films are at 684 and 696 nm, corresponding to bandgap of 1.81 and 1.78 eV, respectively.

Furthermore, the absorption spectra of PDTS-BTA and PDTS-DTBTA films are red-shifted obviously in comparison with that of the D−A copolymers of BTA copolymerized with other weak donor units such as fluorene,[38] carbazole,[37] and BDT.[39,40] The results suggest that enhancing the electron-donating ability of the donor unit to enhance the orbital mixing with the acceptor unit in the D−A copolymers is an effective way for narrowing the bandgap and broadening the absorption of the copolymers.

Hole Mobility. Hole mobility of the two copolymers was measured by the space charge limit current (SCLC) method, as shown in Figure 3. PDTS-DTBTA with thiophene bridges demonstrated a hole mobility of 1.24×10^{-4} cm^2 V^{-1} s^{-1}, which is 3 orders higher than that (3.06×10^{-7} cm^2 V^{-1} s^{-1}) of PDTS-BTA.

Electrochemical Properties. The highest occupied molecular orbital (HOMO) and the lowest unoccupied molecular orbital (LUMO) energy levels of the conjugated polymers are important parameters in determining the V_{oc} and charge transportation efficiency in PSCs, and they can be measured from the onset oxidation and onset reduction potentials of the cyclic voltammograms (CVs) according to the following equations:[45] $E_{HOMO} = -e(\varphi_{ox} + 4.71)$ (eV) and $E_{LUMO} = -e(\varphi_{red} + 4.71)$, where the unit of φ_{ox} and φ_{red} is V vs Ag/Ag$^+$.

Figure 4 shows the cyclic voltammograms of the two copolymers. The onset reduction potential (φ_{red}) and onset oxidation potential (φ_{ox}) of PDTS-BTA are −1.95 and 0.38 V vs Ag/Ag$^+$, respectively, corresponding to LUMO and HOMO energy levels of −2.76 and −5.09 eV, respectively. After introducing the thiophene bridges in PDTS-DTBTA, its LUMO energy level is decreased to −2.81 and its HOMO energy level is slightly up-shifted to −5.05 eV, thus leading to a reduced electrochemical bandgap ($E_g{}^{ec}$) of PDTS-DTBTA. In addition, the $E_g{}^{ec}$ values are ca. 0.5 eV larger than the $E_g{}^{opt}$ values, which is probably due to the exciton binding energy of conjugated polymers.[46] The smaller energy difference (0.46 eV) between $E_g{}^{ec}$ and $E_g{}^{opt}$ for PDTS-DTBTA than that (0.52 eV) for PDTS-BTA indicates that PDTS-DTBTA may have smaller exciton binding energy. The onset oxidation and onset reduction potentials and LUMO and HOMO
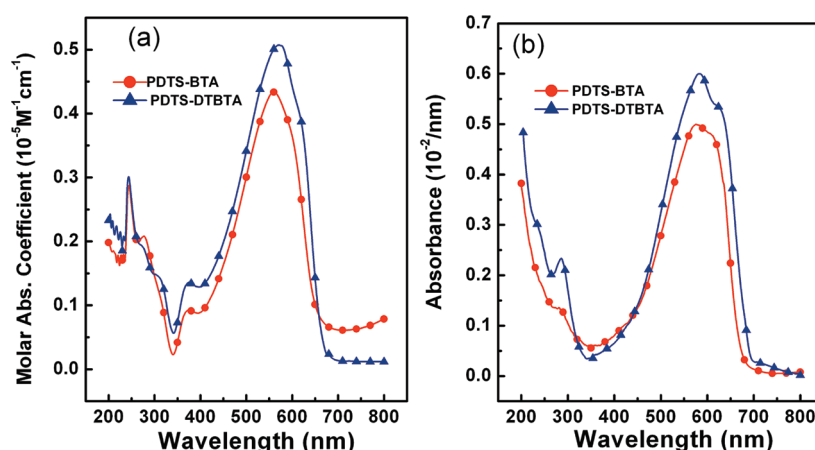
Figure 2. Absorption spectra of the copolymers (a) in dilute chloroform solutions (10^{-5} mol L^{-1}) and (b) in solid films.

Table 2. Optical and Electrochemical Properties of the Polymers

| | UV—vis absorption spectra | | | | cyclic voltammetry | | |
| | solution^a | film^b | | | p-doping | n-doping | |
polymers	λ_{max} (nm)	λ_{max} (nm)	λ_{onset} (nm)	E_g^{opt} (eV)^c	φ_{ox}/HOMO (V)/(eV)	φ_{red}/LUMO (V)/(eV)	E_g^{ec} (eV)
PDTS-BTA	567	576	684	1.81	0.38/−5.09	−1.95/−2.76	2.33
PDTS-DTBTA	575	585	696	1.78	0.34/−5.05	−1.90/−2.81	2.24

^{a} Measured in chloroform solution. ^{b} Cast from chloroform solution. ^{c} Bandgap estimated from the onset wavelength (λ_{edge}) of the optical absorption: $E_g^{opt} = 1240/\lambda_{edge}$.

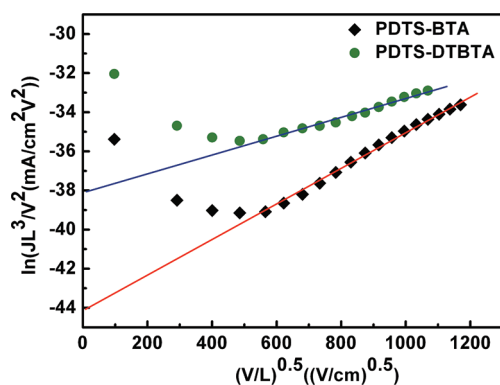**Figure 3.** $\ln(JL^3/V^2)$ vs $(V/L)^{0.5}$ plots of the polymers for the measurement of hole mobility by the SCLC method.

Figure 4. Cyclic voltammograms of PDTS-BTA and PDTS-DTBTA films on a Pt electrode measured in 0.1 mol L^{-1} Bu$_4$NPF$_6$—acetonitrile solutions at a scan rate of 100 mV s^{-1}.

energy levels of the polymers measured are also listed in Table 2 for clear comparison.

Theoretical Calculation. To provide further insight into the fundamentals of molecular architecture, molecular simulation was carried out with a chain length of $n = 1$ at the DFT B3LYP/6-31G(d) level with the Gaussian 03 program package.[47] To simplify the calculation, only one repeating unit of each polymer was subject to the calculation, with alkyl chains replaced by CH$_3$ groups. The simulated electron density distributions and the calculated HOMO and LUMO levels along with optimized geometry are shown in Figure 5.

When benzotriazole was incorporated into the D—A polymers, one must aware the possible steric hindrance brought by the
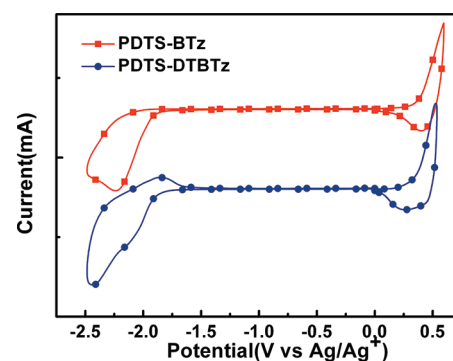
peripheral H atoms and the incorporated solubilizing alkyl chains, which is more significant than in benzothiadiazole. As shown by the optimized geometry (Figure 5b), the insertion of thiophene bridge can well relieve the steric hindrance between the BTA acceptor unit and DTS donor unit and provide improved planarity and greater conjugation length. Recently studies showed that planarity can provide better HOMO/LUMO orbital overlap, thus enhancing the absorption coefficient,[46] which is consistent with our observed higher molar extinction coefficient in PDTS-DTBTA. In addition, it can be seen from Figure 5 and Table 2 that although discrepancies exist between the calculation and experimental results, the trends of variation in the HOMO and LUMO energies, as well as the energy gaps, are similar.
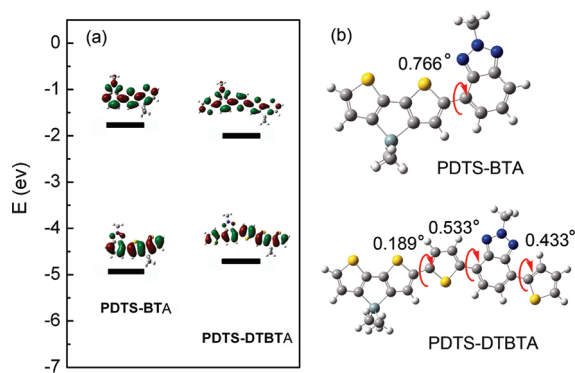
Figure 5. (a) HOMO and LUMO energy levels (eV) and the frontier molecular orbitals obtained from DFT calculations on PDTS-BTA and PDTS-DTBTA with a chain length $n = 1$ at the B3LYP/6-31G* level of theory along with (b) optimized geometry.
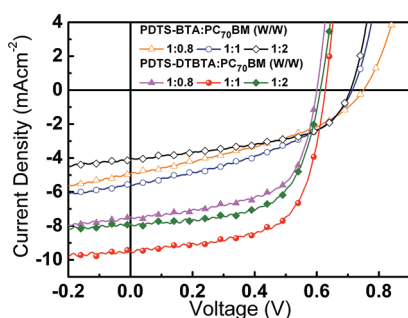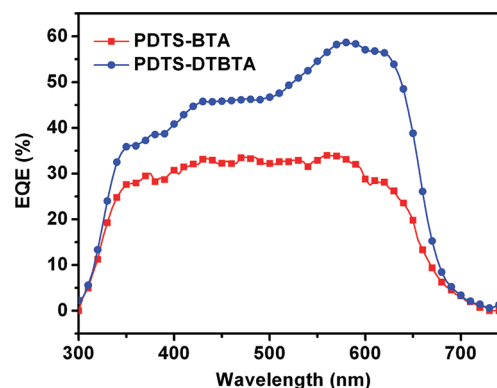

Figure 6. J−V curves of the PSCs based on PDTS-BTA (or PDTS-DTBTA):PC$_{70}$BM with different weight ratios under the illumination of AM1.5, 100 mW cm^{-2}.

Table 3. Photovoltaic Properties of the PSCs Based on the Copolymers with Different Weight Ratios, under the Illumination of AM1.5, 100 mW cm^{-2}

polymers	ratio[a]	V_{oc} (V)	I_{sc} (mA cm^{-2})	FF	PCE (%)
PDTS-BTA	1:0.8	0.75	4.92	0.384	1.42
	1:1	0.71	5.65	0.408	1.64
	1:2	0.71	4.00	0.523	1.49
PDTS-DTBTA	1:0.8	0.60	7.43	0.622	2.77
	1:1	0.63	9.52	0.633	3.80
	1:2	0.61	7.88	0.637	3.06

[a] Polymer/PC$_{70}$BM weight ratio.

Photovoltaic Properties. Polymer solar cells were fabricated from PDTS-BTA or PDTS-DTBTA as donor and (6,6)-phenyl-C$_{70}$-butyric acid methyl ester (PC$_{70}$BM) as acceptor with a general device structure of ITO/PEDOT:PSS/polymer:PC$_{70}$BM/Ca(20 nm)/Al(80 nm). PC$_{70}$BM was chosen as the acceptor because it possesses strong absorption in the visible region from 440 to 530 nm.[48] To balance the absorbance and the charge transporting network of the photoactive layer, the weight ratios of copolymer and PC$_{70}$BM were varied from 1:0.8 to 1:2. Figure 6 shows the J−V curves of the PSCs under the illumination of AM1.5, 100 mW cm^{-2}. The corresponding photovoltaic parameters of the devices are summarized in Table 3. The


Figure 7. EQE curves of the photovoltaic cells with (polymer:PC$_{70}$BM = 1:1) as the active layer.

V_{oc} for the optimized PSC based on PDTS-BTA:PC$_{70}$BM blend was 0.71 V, which is 0.08 V higher than that (0.63 V) of the optimized PSC based on PDTS-DTBTA, benefiting from its lower lying HOMO energy level. The larger V_{oc} difference (0.08 V) than that (0.04 eV) of their HOMO levels difference is due probably to the influence of other factors on the V_{oc}, such as morphology and carrier recombination rate, etc. Also, it worth noting that J_{sc} is strongly affected by the concentration of PC$_{70}$BM in the blend. A higher concentration of PC$_{70}$BM should favor the formation of the interpenetrated networks of the fullerene acceptor, which in turn favors the effective charge separation and charge transportation. Increasing of the PC$_{70}$BM concentration over the weight ratio of 1:1 resulted in decrease of the J_{sc} and PCE values of the PSCs, probably due to the reduction of the amount of polymer donor, which results in the reduction of absorption and hole transporting ability of the active layer. Thus, in both cases, a 1:1 weight ratio seems to be the optimal ratio to form the interpenetrated networks for effective charge separation and transportation.

At the optimal donor/acceptor weight ratio, the PSC based on PDTS-BTA demonstrates a J_{sc} of 5.65 mA cm^{-2}, a V_{oc} of 0.71 V, a FF of 0.408, and PCE of 1.64%. The PSC based on PDTS-DTBTA shows a better photovoltaic performance with J_{sc} of 9.52 mA cm^{-2}, V_{oc} of 0.63 V, FF of 0.63, and PCE of 3.80%. In comparison with PDTS-BTA, the larger molar extinction coefficients of PDTS-DTBTA and higher hole mobility along with slightly better overlap of absorption spectrum with the solar spectrum can account in part for the increase in J_{sc}, as revealed by incident photon to current efficiency (IPCE) spectra. As shown in Figure 7, the IPCE curve of the PSC based on PDTS-DTBTA:PC$_{70}$BM covers a broad wavelength range from 300 to 700 nm with the maximum EQE value of 60% at ca. 580 nm, higher than that of PDTS-BTA.

Morphology. The morphologies of the blend films at the optimal weight ratio were investigated by atomic force microscopy (AFM). As shown in Figure 8, the blend films demonstrated different phase separation state with root-mean-square (rms) roughness of 0.651 nm for PDTS-BTA and 1.140 nm for PDTS-DTBTA, indicating different miscibility between the copolymers and PC$_{70}$BM. The large domain size for PDTS-DTBTA suggested that even better device performance can be expected by further device engineering, such as thermal annealing, solvent annealing, and additives to promote proper phase separation.
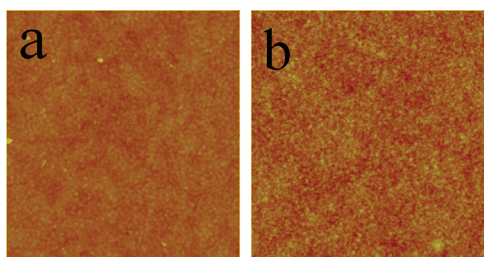
Figure 8. Tapping mode AFM topography images ($5 \times 5 \ \mu m^2$) of the 1:1 (weight ratio) composite films of (a) PDTS-BTA/PC$_{70}$BM and (b) PDTS-DTBTA/PC$_{70}$BM.

CONCLUSION

Two low bandgap D—A copolymers based on DTS donor unit and BTA acceptor unit, PDTS-BTA and PDTS-DTBTA, were synthesized by a palladium(0)-catalyzed Stille coupling reaction. The polymers exhibit good solubility in common organic solvents and good thermal stability. In comparison with PDTS-BTA, PDTS-DTBTA with thiophene bridges between the DTS donor unit and the BDT acceptor unit shows higher molar absorptivity, broader absorption band, lower bandgap, higher hole mobility of $1.24 \times 10^{-4} \ cm^2 \ V^{-1} \ s^{-1}$, and better photovoltaic performance. The PCE based on PDTS-DTBTA:PC$_{70}$BM = 1:1 (w/w) reached 3.80% with $V_{oc} = 0.63$ V, $J_{sc} = 9.52 \ mA \ cm^{-2}$, and FF = 0.63, under the illumination of AM1.5, 100 mW/cm^2. The results indicate that PDTS-DTBTA is a promising polymer donor for future application of PSCs.

AUTHOR INFORMATION

Corresponding Author

*E-mail: liyf@iccas.ac.cn (Y.L.), zgzhangwhu@iccas.ac.cn (Z.Z.).

ACKNOWLEDGMENT

REFERENCES

(1) Yu, G.; Gao, J.; Hummelen, J. C.; Wudl, F.; Heeger, A. J. *Science* **1995**, *270*, 1789.

(2) Thompson, B. C.; Fréchet, J. M. J. *Angew. Chem., Int. Ed.* **2008**, *47*, 58.

(3) Chen, J.; Cao, Y. *Acc. Chem. Res.* **2009**, *42*, 1709.

(4) Cheng, Y.-J.; Yang, S.-H.; Hsu, C.-S. *Chem. Rev.* **2009**, *109*, 5868.

(5) Chen, G.-Y.; Cheng, Y.-H.; Chou, Y.-J.; Su, M.-S.; Chen, C.-M.; Wei, K.-H. *Chem. Commun.* **2011**, *47*, 5064.

(6) Shi, Q.; Fan, H.; Liu, Y.; Hu, W.; Li, Y.; Zhan, X. *J. Phys. Chem. C* **2010**, *114*, 16843.

(7) Lee, S. K.; Cho, J. M.; Goo, Y.; Shin, W. S.; Lee, J.-C.; Lee, W.-H.; Kang, I.-N.; Shim, H.-K.; Moon, S.-J. *Chem. Commun.* **2011**, *47*, 1791.

(8) Zhou, E.; Nakamura, M.; Nishizawa, T.; Zhang, Y.; Wei, Q.; Tajima, K.; Yang, C.; Hashimoto, K. *Macromolecules* **2008**, *41*, 8302.

(9) Huang, F.; Chen, K.-S.; Yip, H.-L.; Hau, S. K.; Acton, O.; Zhang, Y.; Luo, J.; Jen, A. K. Y. *J. Am. Chem. Soc.* **2009**, *131*, 13886.

(10) Zhang, Z.-G.; Liu, Y.-L.; Yang, Y.; Hou, K.; Peng, B.; Zhao, G.; Zhang, M.; Guo, X.; Kang, E.-T.; Li, Y. *Macromolecules* **2010**, *43*, 9376.

(11) Zhang, Z.-G.; Fan, H.; Min, J.; Zhang, S.; Zhang, J.; Zhang, M.; Guo, X.; Zhan, X.; Li, Y. *Polym. Chem.* **2011**, *2*, 1678.

(12) Zhang, Z.-G.; Zhang, K.-L.; Liu, G.; Zhu, C.-X.; Neoh, K.-G.; Kang, E.-T. *Macromolecules* **2009**, *42*, 3104.

(13) He, Z.; Zhang, C.; Xu, X.; Zhang, L.; Huang, L.; Chen, J.; Wu, H.; Cao, Y. *Adv. Mater.* **2011**, *23*, 3086.

(14) Wang, M.; Hu, X.; Liu, P.; Li, W.; Gong, X.; Huang, F.; Cao, Y. *J. Am. Chem. Soc.* **2011**, *133*, 9638.

(15) Huo, L.; Guo, X.; Zhang, S.; Li, Y.; Hou, J. *Macromolecules* **2011**, *44*, 4035–4037.

(16) (a) Zhang, M.; Guo, X.; Li, Y. *Adv. Energy Mater.* **2011**, *1*, 557. (b) Zhang, Z.-G.; Min, J.; Zhang, S. Y.; Zhang, J.; Li, Y. F. *Chem. Commun.* **2011**, *47*, 9474.

(17) Blouin, N.; Michaud, A.; Leclerc, M. *Adv. Mater.* **2007**, *19*, 2295.

(18) Zhou, H.; Yang, L.; Stoneking, S.; You, W. *ACS Appl. Mater. Interfaces* **2010**, *2*, 1377.

(19) Chen, Y.-C.; Yu, C.-Y.; Fan, Y.-L.; Hung, L.-I.; Chen, C.-P.; Ting, C. *Chem. Commun.* **2010**, *46*, 6503.

(20) Chen, C.-P.; Chan, S.-H.; Chao, T.-C.; Ting, C.; Ko, B.-T. *J. Am. Chem. Soc.* **2008**, *130*, 12828.

(21) Hou, J.; Chen, H.-Y.; Zhang, S.; Li, G.; Yang, Y. *J. Am. Chem. Soc.* **2008**, *130*, 16144.

(22) Ding, J.; Song, N.; Li, Z. *Chem. Commun.* **2010**, *46*, 8668.

(23) Wang, J.-Y.; Hau, S. K.; Yip, H.-L.; Davies, J. A.; Chen, K.-S.; Zhang, Y.; Sun, Y.; Jen, A. K. Y. *Chem. Mater.* **2010**, *23*, 765.

(24) Ashraf, R. S.; Chen, Z.; Leem, D. S.; Bronstein, H.; Zhang, W.; Schroeder, B.; Geerts, Y.; Smith, J.; Watkins, S.; Anthopoulos, T. D.; Sirringhaus, H.; de Mello, J. C.; Heeney, M.; McCulloch, I. *Chem. Mater.* **2010**, *23*, 768.

(25) Zhu, Z.; Waller, D.; Gaudiana, R.; Morana, M.; Mühlbacher, D.; Scharber, M.; Brabec, C. *Macromolecules* **2007**, *40*, 1981.

(26) Wienk, M. M.; Turbiez, M.; Gilot, J.; Janssen, R. A. J. *Adv. Mater.* **2008**, *20*, 2556.

(27) Zhou, E.; Wei, Q.; Yamakawa, S.; Zhang, Y.; Tajima, K.; Yang, C.; Hashimoto, K. *Macromolecules* **2010**, *43*, 821.

(28) Ong, K.-H.; Lim, S.-L.; Tan, H.-S.; Wong, H.-K.; Li, J.; Ma, Z.; Moh, L. C. H.; Lim, S.-H.; de Mello, J. C.; Chen, Z.-K. *Adv. Mater.* **2011**, *23*, 1409.

(29) Zhou, H.; Yang, L.; Price, S. C.; Knight, K. J.; You, W. *Angew. Chem., Int. Ed.* **2010**, *49*, 7992.

(30) Zhou, E.; Yamakawa, S.; Zhang, Y.; Tajima, K.; Yang, C.; Hashimoto, K. *J. Mater. Chem.* **2009**, *19*, 7730.

(31) (a) Wang, E.; Hou, L.; Wang, Z.; Hellström, S.; Zhang, F.; Inganäs, O.; Andersson, M. R. *Adv. Mater.* **2010**, *22*, 5240. (b) Zhou, E.; Cong, J.; Tajima, K.; Hashimoto, K. *Chem. Mater.* **2010**, *22*, 4890.

(32) (a) Piliego, C.; Holcombe, T. W.; Douglas, J. D.; Woo, C. H.; Beaujuge, P. M.; Fréchet, J. M. J. *J. Am. Chem. Soc.* **2010**, *132*, 7595. (b) Zhou, E.; Cong, J.; Tajima, K.; Yang, C.; Hashimoto, K. *Macromol. Chem. Phys.* **2011**, *212*, 305.

(33) Zou, Y.; Najari, A.; Berrouard, P.; Beaupré, S.; Réda Aïch, B.; Tao, Y.; Leclerc, M. *J. Am. Chem. Soc.* **2010**, *132*, 5330.

(34) Zhang, G.; Fu, Y.; Zhang, Q.; Xie, Z. *Chem. Commun.* **2010**, *46*, 4997.

(35) Guo, X.; Xin, H.; Kim, F. S.; Liyanage, A. D. T.; Jenekhe, S. A.; Watson, M. D. *Macromolecules* **2010**, *44*, 269.

(36) Balan, A.; Baran, D.; Toppare, L. *Polym. Chem.* **2011**, *2*, 1029.

(37) Peng, B.; Najari, A.; Liu, B.; Berrouard, P.; Gendron, D.; He, Y.; Zhou, K.; Zou, Y.; Leclerc, M. *Macromol. Chem. Phys.* **2010**, *211*, 2026.

(38) Liu, B.; Ye, S.; Zou, Y.; Peng, B.; He, Y.; Zhou, K. *Macromol. Chem. Phys.* **2011**, *212*, 1489.

(39) Zhang, Z.; Peng, B.; Liu, B.; Pan, C.; Li, Y.; He, Y.; Zhou, K.; Zou, Y. *Polym. Chem.* **2010**, *1*, 1441.

(40) Price, S. C.; Stuart, A. C.; Yang, L.; Zhou, H.; You, W. *J. Am. Chem. Soc.* **2011**, *133*, 4625.

(41) Chu, T.-Y.; Lu, J.; Beaupré, S.; Zhang, Y.; Pouliot, J.-R. M.; Wakim, S.; Zhou, J.; Leclerc, M.; Li, Z.; Ding, J.; Tao, Y. *J. Am. Chem. Soc.* **2011**, *133*, 4250.

(42) Carsten, B.; He, F.; Son, H. J.; Xu, T.; Yu, L. *Chem. Rev.* **2011**, *111*, 1493.

(43) Zhou, H.; Yang, L.; Xiao, S.; Liu, S.; You, W. *Macromolecules* **2009**, *43*, 811.

(44) Subramaniyan, S.; Xin, H.; Kim, F. S.; Shoaee, S.; Durrant, J. R.; Jenekhe, S. A. *Adv. Energy Mater.* **2011**, DOI: 10.1002/aenm.201100215.

(45) Sun, Q.; Wang, H.; Yang, C.; Li, Y. *J. Mater. Chem.* **2003**, *13*, 800.

(46) Mondal, R.; Ko, S.; Norton, J. E.; Miyaki, N.; Becerril, H. A.; Verploegen, E.; Toney, M. F.; Bredas, J.-L.; McGehee, M. D.; Bao, Z. *J. Mater. Chem.* **2009**, *19*, 7195.

(47) Gaussian 03: Frisch, M. J.; Trucks, G. W.; Schlegel, H. B.; Scuseria, G. E.; Robb, M. A.; Cheeseman, J. R.; Montgomery, J. A.; Vreven, J., T.; Kudin, K. N.; Burant, J. C.; Millam, J. M.; Iyengar, S. S.; Tomasi, J.; Barone, V.; Mennucci, B.; Cossi, M.; Scalmani, G.; Rega, N.; Petersson, G. A.; Nakatsuji, H.; Hada, M.; Ehara, M.; Toyota, K.; Fukuda, R.; Hasegawa, J.; Ishida, M.; Nakajima, T.; Honda, Y.; Kitao, O.; Nakai, H.; Klene, M.; Li, X.; Knox, J. E.; Hratchian, H. P.; Cross, J. B.; Bakken, V.; Adamo, C.; Jaramillo, J.; Gomperts, R.; Stratmann, R. E.; Yazyev, O.; Austin, A. J.; Cammi, R.; Pomelli, C.; Ochterski, J. W.; Ayala, P. Y.; Morokuma, K.; Voth, G. A.; Salvador, P.; Dannenberg, J. J.; G., Z. V.; Dapprich, S.; Daniels, A. D.; Strain, M. C.; Farkas, O.; Malick, D. K.; Rabuck, A. D.; Raghavachari, K.; Foresman, J. B.; Ortiz, J. V.; Cui, Q.; Baboul, A. G.; Clifford, S.; Cioslowski, J.; Stefanov, B. B.; Liu, G.; Liashenko, A.; Piskorz, P.; Komaromi, I.; Martin, R. L.; Fox, D. J.; Keith, T.; Al-Laham, M. A.; Peng, C. Y.; Nanayakkara, A.; Challacombe, M.; Gill, P. M. W.; Johnson, B.; Chen, W.; Wong, M. W.; Gonzalez, C.; Pople, J. A. Gaussian, Inc.: Wallingford, CT, 2004.

(48) He, Y. J.; Li, Y. F. *Phys. Chem. Chem. Phys.* **2011**, *13*, 1970.